Valence and magnetic ordering in the $Yb_5Si_xGe_{4-x}$ pseudobinary system

C. J. Voyer,[1] D. H. Ryan,[1] Kyunghan Ahn,[2,3] Karl A. Gschneidner, Jr.,[2,3] and V. K. Pecharsky[2,3]
[1]*Centre for the Physics of Materials and Physics Department, McGill University, Montréal, QC, H3A 2T8, Canada*
[2]*Ames Laboratory of the United States Department of Energy, Iowa State University, Ames, Iowa 50011-3020, USA*
[3]*Department of Materials Science and Engineering, Iowa State University, Ames, Iowa 50011-2300, USA*
(Received 20 December 2005; revised manuscript received 3 March 2006; published 18 May 2006)

$Yb_5Si_xGe_{4-x}$ has been studied using ^{170}Yb Mössbauer spectroscopy. Ytterbium is present as both Yb^{2+} and Yb^{3+} in essentially equal amounts. The Yb^{3+} moments order below ~1.7 K for all x, and extrapolation of the hyperfine field to zero temperature yields Yb^{3+} moments of $2.1\pm0.2\mu_B$. Despite the composition independent structure and valence balance in $Yb_5Si_xGe_{4-x}$, we find that the Yb^{3+} ordering is quite complex for $x=1,2,3$ and that there is a marked jump in T_N between $x=3$ and $x=3.5$.

DOI: 10.1103/PhysRevB.73.174422 PACS number(s): 76.80.+y, 75.20.En, 75.20.Hr, 75.30.Kz

I. INTRODUCTION

Following the discovery of a giant magnetocaloric effect (GMCE) in $Gd_5Si_2Ge_2$ (Ref. 1) that is associated with a coupled first-order magnetic and structural transition,[2] the R_5X_4 (R=Y, La-Lu; X=Si,Ge,Sn) family has come under intensive study in order to understand, and ultimately exploit, this remarkable phenomenon. To this end, phase relationships and structural data have now been obtained for about half of the $R_5Si_xGe_{4-x}$ pseudobinary systems[3] (Y,[4] Pr,[5] Nd,[6] Gd,[7–9] Tb,[10] Er,[11] and Yb[12]), while magnetostructural transitions have been identified in $Nd_5Si_{2.4}Ge_{1.6}$,[13] $Gd_5Si_2Ge_2$,[2] $Tb_5Si_2Ge_2$,[14,15] Gd_5Ge_4,[16] and Gd_5Sn_4.[17]

With the accumulation of systematic structural data, it becomes possible to speculate on the influences affecting the extremely delicate balance between magnetic and structural energies in the R_5X_4 systems. Two quite natural parameters are emerging. The first is the radius of the rare earth, r_R, compared with r_X, the weighted average of the alloying elements (Si,Ge,Sn). As the ratio r_R/r_X decreases, there is an evolution in structure from the tetragonal Zr_5Si_4-type (T) through orthorhombic Gd_5Si_4-type (O-I), monoclinic $Gd_5Si_2Ge_2$-type (M) to the orthorhombic Sm_5Ge_4-type (O-II).[4] The lanthanide contraction then dominates the form of the structural phase diagram in the paramagnetic state, while thermal contraction and contributions from magnetic ordering can shift the balance and lead to magnetostructural transitions on cooling. The energy differences between the various structures are quite small,[18] so that modest magnetic fields (~2 T drives an O-II→O-I transition in Gd_5Ge_4 at 6 K[16]) or hydrostatic pressures (~8 kbar permits a coupled M→O-I magnetostructural transition at 115 K in $Tb_5Si_2Ge_2$[15]) can induce profound changes in the crystallography and magnetic properties of these materials. The second controlling parameter appears to be the valence electron concentration. Calculations[2,19] have linked optimization of the magnetic energy to an increase in valence electron density on going from the M to O-I structure in $Gd_5Si_2Ge_2$. Changing the valence electron concentration at fixed r_R/r_X in $Gd_5Ga_xGe_{4-x}$ has provided support for this idea, and also led to the discovery of an intermediate orthorhombic Pu_5Rh_4-type structure as progressive Ga substitution drives the valence electron density down and the structure evolves from O-II to O-I.[20] More recently, stabilization of the O-I structure by reduced valence electron density has also been demonstrated by replacing the trivalent lanthanide by divalent calcium in $La_{5-x}Ca_xGe_4$ and $Ce_{5-x}Ca_xGe_4$.[21]

Against this backdrop, the $Yb_5Si_xGe_{4-x}$ system is of particular interest. Yb occurs in two valence states, Yb^{2+} and Yb^{3+}, with very different sizes ($r_{Yb^{2+}}=1.940$ Å, $r_{Yb^{3+}}=1.740$ Å).[22] Furthermore, substituting Si for Ge in $YbMn_2Si_xGe_{2-x}$ drives a valence change from Yb^{2+} to Yb^{3+} (Ref. 23). Thus one might expect both r_R/r_X and valence electron density to play significant roles in defining the room temperature crystallography and hence physical properties of the $Yb_5Si_xGe_{4-x}$ system. Surprisingly, $Yb_5Si_xGe_{4-x}$ was found to adopt the orthorhombic Gd_5Si_4-type (O-I) structure for all x,[12] in contrast to r_R/r_X arguments that would predict either T (for Yb^{2+}) or O-II (for Yb^{3+}). Analysis of magnetic susceptibility data for the series suggests that the Yb atoms are not present in a unique valence state and a 60%:40% Yb^{2+}:Yb^{3+} distribution was inferred. Size considerations would then yield a T→O-I evolution with increasing x, but valence electron density arguments would predict O-I only. Finally, a weak maximum in susceptibility provided indirect evidence for magnetic ordering at quite low temperatures, ranging from 3.2 K at $x=0$ to 2.4 K at $x=4$. Magnetization data at 1.8 K yield reduced Yb moments even when corrected for the large fraction of nonmagnetic Yb^{2+}, suggesting either antiferromagnetic or ferrimagnetic ordering of the Yb^{3+} moments.

Here we report results of a ^{170}Yb Mössbauer spectroscopy study of both valence and magnetic ordering in the $Yb_5Si_xGe_{4-x}$ pseudobinary system. Our direct, microscopic measurements complement the earlier bulk study by Ahn *et al.* and confirm their main conclusions,[12] however, there are a number of differences. We find that the Yb^{2+}:Yb^{3+} ratio is closer to 50%:50%, and that the onset of magnetic order occurs at temperatures about 1 K below those inferred previously from magnetic susceptibility. Finally, despite the apparent uniformity in structure and valence in this system, we find that the magnetic ordering is quite complex. For $x=1$, 2, and 3, there are two distinct Yb^{3+} components that order at separate temperatures, while only one Yb^{3+} component is seen in the end-member materials ($x=0,4$). Furthermore, we observe a clear break in magnetic behavior between $x=3$ and

$x=3.5$ that does not appear to be associated with any crystallographic changes.

II. EXPERIMENTAL METHODS

Four of the $Yb_5Si_xGe_{4-x}$ samples ($x=0$, 2, 3, and 4) used here were studied previously[12] and all sample preparation details along with an extensive discussion of the crystallographic analysis are reported there. Two new samples were prepared specifically for this study using the same methods. A new $x=1$ sample was made as the one from the previous study was not single phased, and the $x=3.5$ sample was prepared in order to better localize the break in magnetic behavior at the silicon-rich end of the phase diagram that was observed during the course of this work. All six samples were checked using neutron diffraction at ambient temperatures on the 800-wire C2 powder diffractometer at the Canadian Neutron Beam Centre, Chalk River, Ontario, to confirm phase identity and purity. $Yb_5Si_xGe_{4-x}$ adopts the orthorhombic (*Pnma* #62) Gd_5Si_4-type (O-I) structure for all x with the twenty ytterbium atoms in the unit cell occupying three distinct sites ($4c$, $8d_1$ and $8d_2$).

A 20 mCi ^{170}Tm source was prepared by neutron activation of ~25 mg of Tm as a 10 wt % alloy in aluminium. The source and sample were mounted vertically in a helium-flow cryostat and the drive was operated in sine mode. The 84.25 keV γ photons used for ^{170}Yb Mössbauer were isolated from the various x rays emitted by the source using a high-purity Ge detector. Calibration of the spectrometer was achieved using a laser interferometer mounted on the back of the drive. Velocities were cross-checked against ^{57}Co/α-Fe at room temperature. This procedure has also been checked at higher velocities than those employed here by recording and fitting the ^{166}Er Mössbauer spectrum of $ErFe_2$ at 5 K.[24] We observed a ^{170}Yb linewidth (half width at half maximum) of 1.33(6) mm/s with the source and a standard sample of YbB_6 at 5.0 K. A calibrated Cernox thermometer was used to monitor the sample temperature and a stability of better than ±0.01 K was observed. Spectra were fitted using a nonlinear least-squares minimization routine with line positions and intensities derived from an exact solution to the full Hamiltonian.

III. RESULTS AND DISCUSSION

Unlike the more commonly used ^{57}Fe and ^{119}Sn Mössbauer isotopes, the 84.25 keV $2^+ \rightarrow 0^+$ transition in ^{170}Yb involves a rotational change at almost constant nuclear volume and so isomer shifts (δ) cannot be used to distinguish valence states in a reliable manner. We do observe a slight increase in δ on going from Yb^{2+} to Yb^{3+}, but at 0.21(7) mm/s, this change is only 16% of our instrumental linewidth and is not a useful indicator of valence.[25] Fortunately, electric field gradients and magnetic ordering make it easy to distinguish the two ytterbium valence states. Yb^{2+} is nonmagnetic with a closed-shell, spherically symmetric $4f^{14}$ electronic configuration. With no $4f$ contribution to the electric field gradient (efg) only the much smaller lattice contribution is present, and Yb^{2+} exhibits quite small quadrupole

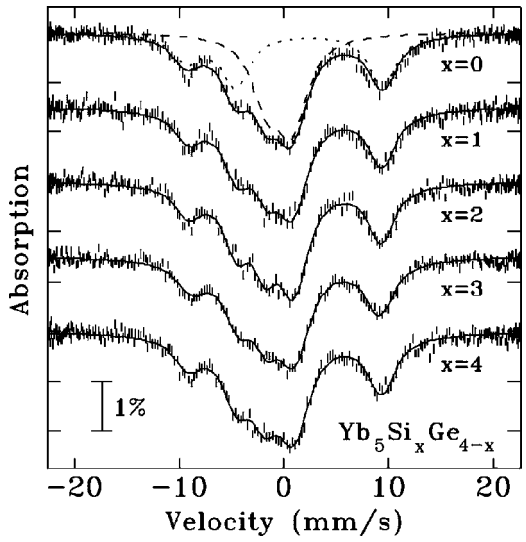

FIG. 1. ^{170}Yb Mössbauer spectra of $Yb_5Si_xGe_{4-x}$ taken at 5.0 K, above their ordering temperatures, showing the central Yb^{2+} quadrupole triplet and an approximately equal-area quadrupole triplet from Yb^{3+} giving lines to the left and right of the central feature. Solid lines are fits described in the text. For $x=0$ we show the form of the Yb^{2+} component (dashed line) and the Yb^{3+} component (dotted line).

interactions (Δ) in a ^{170}Yb Mössbauer spectrum. By contrast, $4f^{13}$ Yb^{3+} has a large $4f$ contribution to the efg and also exhibits magnetic order. As can be seen in Fig. 1, the two valence states are readily distinguished. The central, poorly resolved, triplet is due primarily to Yb^{2+}, while Yb^{3+} gives lines to the left and right of the central feature. The low point symmetries of the three Yb sites could be expected to lead to non axially-symmetric efg's, however, we were unable to resolve a statistically significant contribution for either the Yb^{2+} or the Yb^{3+} component, so the asymmetry parameter (η) was set to zero for the fits presented here.

Mapping spectral areas onto the two valence fractions is not necessarily automatic. For example, when europium changes from divalent to trivalent in $EuMn_2Si_xGe_{2-x}$ with increasing x,[26] the two forms exhibit very different recoil free fractions in the ^{151}Eu Mössbauer spectra as a result of different binding. Examination of spectra for Yb_5Si_4 between 5 K and 40 K yields Debye temperatures of 175(5) K (Yb^{2+}) and 178(8) K (Yb^{3+}) for the two components, with a temperature independent Yb^{2+}:Yb^{3+} ratio of 50.9(1.4):49.1(1.4). We are therefore able to use the spectral area ratio at 5 K as an accurate, direct measure of the two valence populations.

The main parameters derived from fitting the 5 K spectra in Fig. 1 are summarized in Fig. 2. While we do provide a clear confirmation that Yb is present in both valence states and that the Yb^{2+}:Yb^{3+} ratio is composition independent, we find somewhat more Yb^{3+} than was inferred previously[12] [48.4(0.3)% from Mössbauer, averaged across all samples vs 38(2)% from magnetic susceptibility]. The most immediate outcome of this result is that it is not possible to assign half of the Yb ions to a single site, or simple combination of sites, within the O-I structure. It is therefore unlikely that the Yb^{3+} atoms are located only on the Yb3 ($8d_2$) site as previously

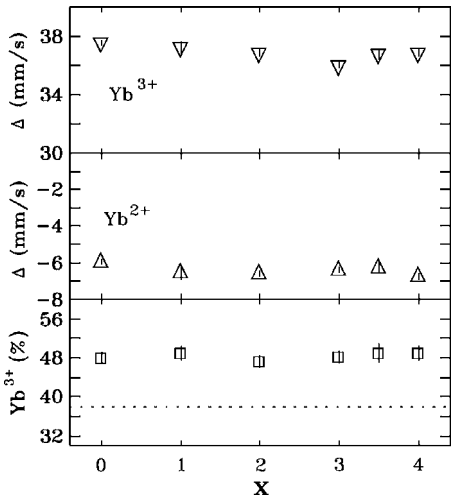

FIG. 2. Summary of fitted parameters for the spectra shown in Fig. 1. Top and middle panels: quadrupole interaction (Δ) for the Yb^{3+} and Yb^{2+} components. Note the factor of six difference in absolute values. Bottom panel: fractional area associated with Yb^{3+} for each of the compounds studied here. Dotted line in lowest panel shows Yb^{3+} fraction estimated from magnetic susceptibility data (Ref. 12).

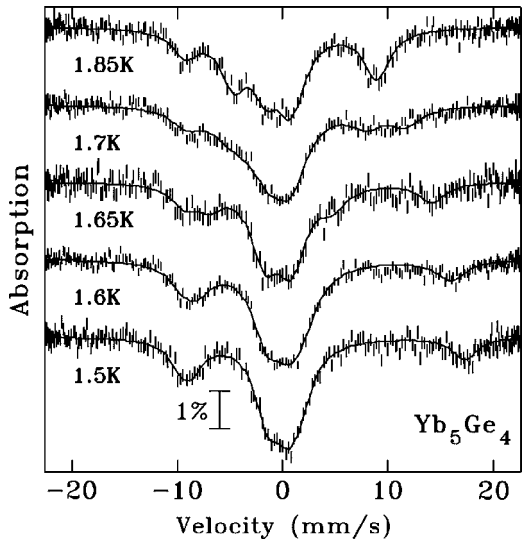

FIG. 3. ^{170}Yb Mössbauer spectra for Yb_5Ge_4 showing the changes associated with magnetic ordering of the Yb^{3+} component below T_N=1.71(1) K. Solid lines are fits to the full Hamiltonian as described in the text.

suggested.[12] While the Yb^{3+} must occur on at least two of the three possible crystallographic sites, we observe only a single Yb^{3+} component in the 5 K spectra. Similarly, we see only a single Yb^{2+} component. Thus the hyperfine environments of the sites occupied by Yb^{2+} and Yb^{3+} are quite similar, and as a result, it is not possible for us to say with any certainty whether the Yb ions with a particular valence prefer one or more sites or are distributed uniformly among the three possible locations. The composition independent structure and valence ratio in this system, coupled with the small changes in hyperfine parameters observed with increasing x, indicate that the effects of replacing Ge by Si are quite minor. It is not surprising therefore, that we also observed no changes in the linewidth, or any other Mössbauer parameter, that could be attributed to the Si/Ge site disorder which must be present for $x \neq 0,4$.

Closer inspection of Δ vs x for the Yb^{3+} component in Fig. 2 reveals an apparent break in the trend between x=3 and x=3.5. While no break is seen in the other Mössbauer parameters or was reported in the earlier crystallographic data,[12] we will show below that there is a significant change in the magnetic ordering in the same composition range.

Cooling Yb_5Ge_4 below 5 K ultimately leads to the onset of magnetic order for the Yb^{3+} ions as can be seen in Fig. 3. As expected, the Yb^{2+} component is not affected by the ordering since it carries no magnetic moment and there is no evidence of a transferred hyperfine field from ordered Yb^{3+} neighbors. More importantly, the Yb^{2+}:Yb^{3+} ratio does not change on cooling, even when the Yb^{3+} component orders. Similar behavior is seen for Yb_5Si_4. As with the paramagnetic spectra in Fig. 1, we are unable to resolve either the Yb^{2+} or the Yb^{3+} component into subspectra, and therefore conclude that the Yb environments remain similar in the ordered state for x=0 and 4. Fits to the Yb^{3+} component indicate that B_{hf} is parallel to the principal axis of the efg in both end member compounds. The absence of any significant change in the observed quadrupole interaction at both the Yb^{2+} and the Yb^{3+} sites suggests that the crystal structure does not change on cooling through T_N, this observation, along with the constant Yb^{2+}:Yb^{3+} ratio confirms the structural and valence stability of the x=0 and 4 compounds.

Fitting the temperature dependence of the hyperfine field $[B_{hf}(T)]$ in Fig. 4 yields an ordering temperature of 1.71(1) K for Yb_5Ge_4, well below the 3.2 K inferred from the maximum in the magnetic susceptibility.[12] Similar behavior is seen in the Yb_5Si_4 compound, where the Yb^{2+}:Yb^{3+} ratio is again stable, and we obtain an ordering temperature of 1.62(1) K, again lower than the 2.4 K derived from susceptibility.[12] As the original magnetic susceptibility data

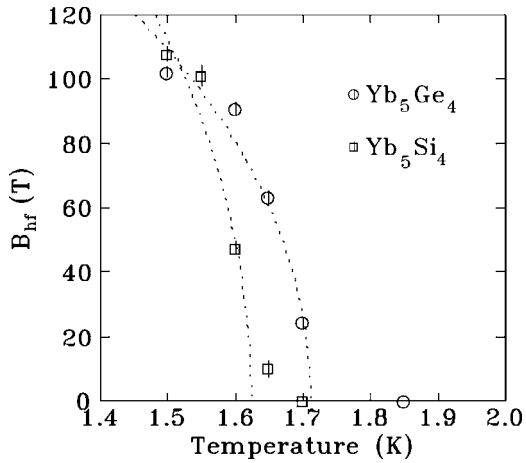

FIG. 4. Temperature dependence of the hyperfine field (B_{hf}) for Yb_5Ge_4 (○) and Yb_5Si_4 (□) showing the onset of magnetic order at 1.71(1) K and 1.62(1) K, respectively. The dotted lines are fits to Brillouin functions used to obtain T_N and the zero-temperature hyperfine field $[B_{hf}(0)]$.

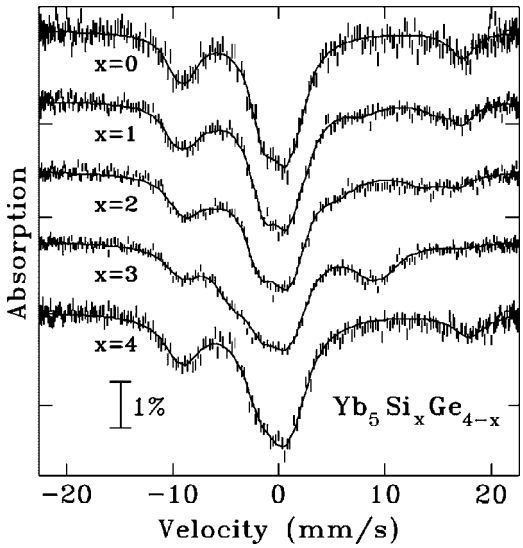

FIG. 5. ^{170}Yb Mössbauer spectra for $Yb_5Si_xGe_{4-x}$ at 1.5 K showing the effects of magnetic ordering on the Yb^{3+} component in each compound. Note the very similar appearance of the spectra for the end members ($x=0,4$) and the more complex behavior evident for $x=1,2,3$. Solid lines are fits to the full Hamiltonian as described in the text.

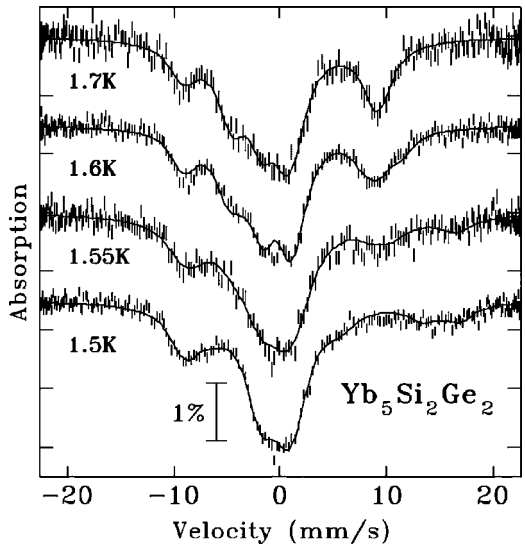

FIG. 6. ^{170}Yb Mössbauer spectra for $Yb_5Si_2Ge_2$ at 1.5 K$<T<$1.7 K showing the changes associated with the magnetic ordering of the Yb^{3+} component. The two magnetic contributions are most visible at 1.5 K and 1.55 K around +15 mm/s. Solid lines are fits to the full Hamiltonian as described in the text.

were taken on heating in a dc field of 50 mT, we have rerun the susceptibility in an ac field of 1 mT at 300 Hz on cooling in zero dc field to see whether the measurement protocol has any effect on the maximum in $\chi(T)$. Our new results were fully consistent with those published earlier for all five compounds common to the two studies ($x=0,1,2,3,4$). We therefore conclude that the maximum in $\chi(T)$ does not mark the onset of magnetic order in these compounds. This serves to underline the advantages of a direct measurement of the magnetic order in situations where the behavior is complex.

Estimating the zero-temperature Yb^{3+} moment for the two end member compounds involves a rather severe extrapolation of our Brillouin fits as we only reach ~90% of T_N. The fits yield 190(15) T and 245(25) T for Yb_5Ge_4 and Yb_5Si_4, respectively, with a weighted average of 210(20) T. Using the conversion factor between B_{hf} and μ_{Yb} of 100 T/μ_B,[27] gives an estimated Yb^{3+} moment of $2.1\pm0.2\mu_B$. While this is much lower than the free-ion Yb^{3+} moment of 4.0 μ_B, it compares well with the ~1.7 μ_B/Yb^{3+} derived from magnetization data taken at 1.8 K[12] (*above* T_N), corrected for our revised $Yb^{2+}:Yb^{3+}$ ratio. The Mössbauer value comes from direct microscopic measurements of B_{hf} made below T_N with no external field. B_{hf} is not affected by the details of magnetic ordering nor does anisotropy play a role. As a result, it more accurately reflects the unperturbed Yb^{3+} moment in these compounds.

Spectra taken at 1.5 K for five of the $Yb_5Si_xGe_{4-x}$ compounds studied here are shown in Fig. 5. In each case, the $Yb^{2+}:Yb^{3+}$ ratio does not change when the Yb^{3+} component orders. The similarity between the Yb_5Ge_4 and Yb_5Si_4 compounds is evident. However, it is also clear from Fig. 5 that the mixed Si/Ge compounds ($x=1,2,3$) exhibit more complex behavior: The Yb^{3+} contribution orders as two distinct subcomponents, one of which appears to correspond to the ~100 T Yb^{3+} component seen in the end member spectra, while the other exhibits a much smaller field. This increased complexity is most clearly seen for $x=2$ where the two subcomponents have approximately equal areas [26.7(2.0)% and 22.8(2.4)%] with fields of 102(3) T and 53(3) T, respectively (Fig. 6). The temperature dependence of B_{hf} for the two Yb^{3+} subcomponents also suggests distinct ordering temperatures of 1.63(2) K and 1.56(2) K for the high and low field contributions, respectively (Fig. 7).

The fitted 1.5 K hyperfine fields, the subcomponent areas, and transition temperatures are summarized in Fig. 8, where it is evident that, despite the apparently simple structure and valence properties of this system, the magnetic ordering exhibits a complex evolution. Replacing Ge by Si leads to a

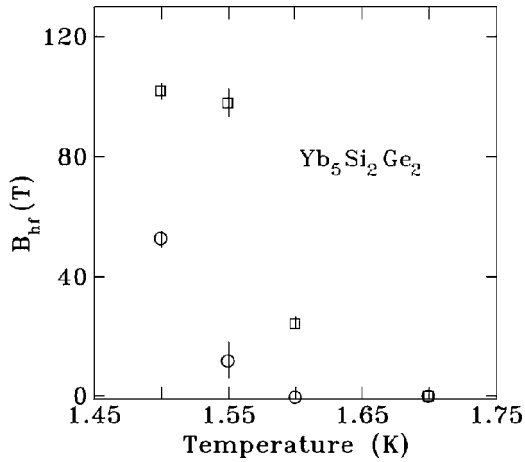

FIG. 7. Temperature dependence of the hyperfine fields (B_{hf}) for $Yb_5Si_2Ge_2$ showing separate ordering for the high-field (□) and low-field (○) subcomponents at 1.63(2) K and 1.56(2) K, respectively.

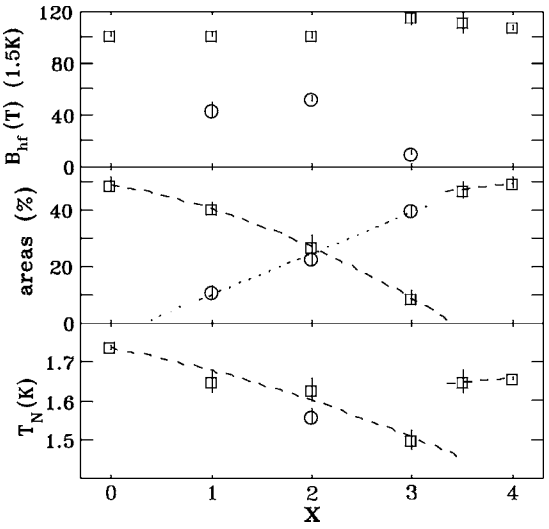

FIG. 8. Fitted values for top: B_{hf} (at 1.5 K), center: areas of the Yb^{3+} component or subcomponents, and bottom: T_N for the Yb^{3+} component or subcomponents, for $Yb_5Si_xGe_{4-x}$. In all cases, the symbols correspond between plots. Dotted and dashed lines are guides to the eye and serve to emphasize the discontinuities between $x=3$ and $x=3.5$.

gradual decline in T_N and the appearance of a low-field, reduced T_N subcomponent. This low-field subcomponent becomes the dominant Yb^{3+} feature by $x=3$ but is entirely absent by $x=3.5$. The discontinuity in the Yb^{3+} spectral areas is also associated with a clear break in $T_N(x)$ as the slow decline in ordering temperature is interrupted by a 10% increase between $x=3$ and $x=3.5$. We emphasize that since the Yb^{2+}:Yb^{3+} area ratio is the same above and below T_N in all six compounds, we are accounting for *all* of the Yb^{3+} in the samples. The absence or presence of the low-field subcomponent is therefore real and cannot be an artefact of missing some fraction of the Yb^{3+} in the sample, nor can it be attributed to a $Yb^{2+} \leftrightarrow Yb^{3+}$ valence conversion.

While the fitted values of T_N shown in Fig. 8 exhibit much the same trend reported previously, namely a slight decrease with increasing x,[12] the actual values found here are about 1 K lower than those inferred previously from the maximum in $\chi(T)$. This discrepancy between the magnetization and Mössbauer results is likely related to anomalies in $M(T)$ often observed above the actual magnetic ordering temperatures in low-field magnetization measurements on $R_5Si_xGe_{4-x}$ compounds.[28] Recent small angle neutron scattering work on $Tb_5Si_2Ge_2$ has linked these anomalies to a short-range magnetic clustering that occurs well above the onset of long range magnetic order.[29] As ^{170}Yb Mössbauer provides a direct, microscopic probe of magnetic ordering, and we observe no indications of relaxation effects, we believe that the values quoted for T_N in Fig. 8 are the real ordering temperatures of these compounds. We also observe a marked break in T_N vs x between $x=3$ and $x=3.5$ that is associated with the disappearance of the low-field Yb^{3+} component, and mirrors the trend in quadrupole interaction vs composition apparent in Fig. 2.

IV. CONCLUSIONS

^{170}Yb Mössbauer spectra of $Yb_5Si_xGe_{4-x}$ taken between 1.5 K and 40 K show that Yb is present as Yb^{2+} and Yb^{3+} in nearly equal amounts [51.6(0.3)% and 48.4(0.3)%, respectively] and that this balance is independent of temperature and composition. Magnetic order develops below 1.7 K with the zero temperature Yb^{3+} moments estimated to be $2.1\pm0.2\mu_B$ for $x=0$ and 4. These results are in fair agreement with those reported by Ahn *et al.*[12] Intermediate compositions ($x=1,2,3$) exhibit two distinct ordered Yb^{3+} subcomponents which appear to have separate ordering temperatures, furthermore, we observe a clear break in magnetic behavior between $x=3$ and $x=3.5$, that does not appear to be associated with any crystallographic changes.

Final confirmation of ordering and magnetic structures will come from neutron diffraction data. While neutrons are insensitive to valence, the diffraction data should allow us to determine the amount and location of the Yb^{3+} ions in $Yb_5Si_xGe_{4-x}$ as only Yb^{3+} carries a magnetic moment.

ACKNOWLEDGMENTS

This work was supported by grants from the Natural Sciences and Engineering Research Council of Canada and Fonds pour la formation de chercheurs et l'aide à la recherche, Québec. Source activations were carried out by M. Butler at the McMaster Nuclear Reactor (MNR), Hamilton, Ontario. D.H.R. and C.J.V. would like to acknowledge many useful discussions with J. M. Cadogan (UNSW) during the course of this work. Work at Ames Laboratory, Iowa State University was supported by the Office of Basic Energy Sciences, Materials Sciences Division of the U.S. Department of Energy under Contract No. W-7405-ENG-82.

[1] V. K. Pecharsky and K. A. Gschneidner, Jr., Phys. Rev. Lett. **78**, 4494 (1997).
[2] W. Choe, V. K. Pecharsky, A. O. Pecharsky, K. A. Gschneidner, Jr., V. G. Young, and G. J. Miller, Phys. Rev. Lett. **84**, 4617 (2000).
[3] K. A. Gschneidner, Jr., V. K. Pecharsky, A. O. Pecharsky, V. V. Ivtchenko, and E. M. Levin, J. Alloys Compd. **303-304**, 214 (2000).
[4] A. O. Pecharsky, V. K. Pecharsky, and K. A. Gschneidner, Jr., J. Alloys Compd. **379**, 127 (2004).
[5] H. F. Yang, G. Rao, W. G. Chu, G. Liu, Z. Ouyang, and J. K. Liang, J. Alloys Compd. **339**, 189 (2002).
[6] H. F. Yang, G. Rao, G. Liu, Z. Ouyang, W. Liu, X. M. Feng, W. G. Chu, and J. K. Liang, J. Alloys Compd. **346**, 190 (2002).
[7] V. K. Pecharsky and K. A. Gschneidner, Jr., J. Alloys Compd. **260**, 98 (1997).
[8] L. Morellon, J. Blasco, P. A. Algarabel, and M. R. Ibarra, Phys. Rev. B **62**, 1022 (2000).

[9] A. O. Pecharsky, K. A. Gschneidner, Jr., V. K. Pecharsky, and C. E. Schindler, J. Alloys Compd. **338**, 126 (2002).
[10] C. Ritter, L. Morellon, P. A. Algarabel, C. Magen, and M. R. Ibarra, Phys. Rev. B **65**, 094405 (2002).
[11] A. O. Pecharsky, K. A. Gschneidner, Jr., V. K. Pecharsky, D. L. Schlagel, and T. A. Lograsso, Phys. Rev. B **70**, 144419 (2004).
[12] K. Ahn, A. O. Tsokol, Y. Mozharivskyj, K. A. Gschneidner, Jr., and V. K. Pecharsky, Phys. Rev. B **72**, 054404 (2005).
[13] C. Magen, L. Morellon, P. A. Algarabel, M. R. Ibarra, C. Ritter, A. O. Pecharsky, K. A. Gschneidner, Jr., and V. K. Pecharsky, Phys. Rev. B **70**, 224429 (2004).
[14] L. Morellon, C. Ritter, C. Magen, P. A. Algarabel, and M. R. Ibarra, Phys. Rev. B **68**, 024417 (2003).
[15] L. Morellon, Z. Arnold, C. Magen, C. Ritter, O. Prokhnenko, Y. Skorokhod, P. A. Algarabel, M. R. Ibarra, and J. Kamarad, Phys. Rev. Lett. **93**, 137201 (2004).
[16] V. K. Pecharsky, A. P. Holm, K. A. Gschneidner, Jr., and R. Rink, Phys. Rev. Lett. **91**, 197204 (2003).
[17] D. H. Ryan, M. Elouneg-Jamróz, J. van Lierop, Z. Altounian, and H. B. Wang, Phys. Rev. Lett. **90**, 117202 (2003).
[18] G. D. Samolyuk and V. P. Antropov, J. Appl. Phys. **97**, 10A310 (2005).
[19] V. K. Pecharsky, G. D. Samolyuk, V. P. Antropov, A. O. Pecharsky, and K. A. Gschneidner, Jr., J. Solid State Chem. **171**, 57 (2003).
[20] Y. Mozharivsky, W. Choe, A. O. Pecharsky, and G. J. Miller, J. Am. Chem. Soc. **125**, 15183 (2003).
[21] L. M. Wu, S. H. Kim, and D. K. Seo, J. Am. Chem. Soc. **127**, 15682 (2005).
[22] K. A. Gschneidner, Jr., *The Rare Earths*, 1st ed. (Wiley, New York, 1961).
[23] D. H. Ryan, J. M. Cadogan, and A. V. J. Edge, J. Phys.: Condens. Matter **16**, 6129 (2003).
[24] D. H. Ryan, J. M. Cadogan, and R. Gagnon, Phys. Rev. B **68**, 014413 (2003).
[25] E. R. Bauminger, G. M. Kalvius, and I. Nowik, *Mössbauer Isomer Shifts*, 1st ed. (North-Holland, Amsterdam, 1978).
[26] I. Nowik, I. Felner, and E. R. Bauminger, Phys. Rev. B **55**, 3033 (1997).
[27] A. Abragam and B. Bleaney, *Electronic Paramagnetic Resonance of Transition Ions* (Clarendon, Oxford, 1976).
[28] J. Szade and G. Skorek, J. Magn. Magn. Mater. **196-197**, 699 (1999).
[29] C. Magen, P. A. Algarabel, L. Morellon, J. P. Araújo, C. Ritter, M. R. Ibarra, A. M. Pereira, and J. B. Sousa, Phys. Rev. Lett. **96**, 167201 (2006).